

RESEARCH

Open Access



# Metabolic engineering of *Komagataella phaffii* for the efficient utilization of methanol

Yuanyuan Wang<sup>1†</sup>, Ruisi Li<sup>1†</sup>, Fengguang Zhao<sup>2</sup>, Shuai Wang<sup>1</sup>, Yaping Zhang<sup>1</sup>, Dexun Fan<sup>1</sup> and Shuangyan Han<sup>1\*</sup>

## Abstract

**Background** *Komagataella phaffii*, a type of methanotrophic yeast, can use methanol, a favorable non-sugar substrate in eco-friendly bio-manufacturing. The dissimilation pathway in *K. phaffii* leads to the loss of carbon atoms in the form of CO<sub>2</sub>. However, the  $\Delta$ FLD strain, engineered to lack formaldehyde dehydrogenase—an essential enzyme in the dissimilation pathway—displayed growth defects when exposed to a methanol-containing medium.

**Results** Inhibiting the dissimilation pathway triggers an excessive accumulation of formaldehyde and a decline in the intracellular NAD<sup>+</sup>/NADH ratio. Here, we designed dual-enzyme complex with the alcohol oxidase1/dihydroxyacetone synthase1 (Aox1/Das1), enhancing the regeneration of the formaldehyde receptor xylulose-5-phosphate (Xu5P). This strategy mitigated the harmful effects of formaldehyde accumulation and associated toxicity to cells. Concurrently, we elevated the NAD<sup>+</sup>/NADH ratio by overexpressing isocitrate dehydrogenase in the TCA cycle, promoting intracellular redox homeostasis. The OD<sub>600</sub> of the optimized combination of the above strategies, strain DF02-1, was 4.28 times higher than that of the control strain DF00 ( $\Delta$ FLD, *HIS4*<sup>+</sup>) under 1% methanol. Subsequently, the heterologous expression of methanol oxidase Mox from *Hansenula polymorpha* in strain DF02-1 resulted in the recombinant strain DF02-4, which displayed a growth at an OD<sub>600</sub> 4.08 times higher than that the control strain DF00 in medium containing 3% methanol.

**Conclusions** The reduction of formaldehyde accumulation, the increase of NAD<sup>+</sup>/NADH ratio, and the enhancement of methanol oxidation effectively improved the efficient utilization of a high methanol concentration by strain  $\Delta$ FLD strain lacking formaldehyde dehydrogenase. The modification strategies implemented in this study collectively serve as a foundational framework for advancing the efficient utilization of methanol in *K. phaffii*.

**Keywords** *Komagataella Phaffii*, Methanol, Xu5P, Formaldehyde, NAD<sup>+</sup>/NADH

<sup>†</sup>Yuanyuan Wang and Ruisi Li contributed equally to this work.

\*Correspondence:

Shuangyan Han  
syhan@scut.edu.cn

<sup>1</sup>Guangdong Key Laboratory of Fermentation and Enzyme Engineering, School of Biology and Biological Engineering, South China University of Technology, Guangzhou, China

<sup>2</sup>School of Light Industry and Engineering, South China University of Technology, Guangzhou, China



## Introduction

Methanol, an important bulk chemical, is industrially produced from natural gas and various renewable resources through an intermediate syngas [1]. Ongoing research explores the synthesis of methanol from CO<sub>2</sub>, considered a promising avenue for mitigating global warming and achieving global carbon neutrality on a global scale [2]. As a non-food organic C1 feedstock, methanol avoids competition with human food sources and stands out as a carbon substitute for sugar in eco-friendly bio-manufacturing processes [3]. Its appeal lies in both its low cost and abundant sources [4]. Furthermore, owing to its higher degree of reduction compared to the majority of sugars [5], methanol can serve as a primary or supplementary carbon source for the production of reducing chemicals, including alcohols, organic acids, and hydrocarbons, with the expectation of higher yields.

Nature encompasses two main categories of methylotrophic microorganisms: methylotrophic bacteria and methylotrophic yeasts. These organisms possess the natural ability to utilize C1 compounds, such as methanol, as substrates for growth and metabolism [6]. Numerous studies have been conducted on the utilization of methanol by various industrial microorganisms, including *Escherichia coli* [7], *Corynebacterium glutamicum* [8], *Saccharomyces cerevisiae* [9], and *Yarrowia lipolytica* [10]. These investigations involve the introduction and optimization of heterologous methanol assimilation pathways. *Komagataella phaffii* (syn *Pichia pastoris*) [11], a native methanotrophic yeast, is widely used in the industry, utilizing methanol as a carbon source for the production of high value-added products, such as heterologous proteins and biochemicals. This preference is attributed to advantages like strain stability and high cell density fermentation [12, 13]. Despite its widespread use, *K. phaffii* encounters limitations in methanol-based bio-industry due to the inherent toxicity of methanol and its intermediate metabolite formaldehyde to cells, coupled with the loss of carbon atoms in the form of CO<sub>2</sub> formed through the dissimilation pathway [12]. Addressing these challenges, Cai et al. [14] overexpressed the endogenous gene *DAS2* in *K. phaffii*, which further drives formaldehyde assimilation, reduces formaldehyde accumulation, and increases biomass fatty acid yield. In general, there is a relative scarcity of studies focused on the efficient methanol utilization in *K. phaffii*.

In a previous study [15], our efforts to mitigate the loss of carbon atoms in the dissimilation pathway of *K. phaffii* involved knocking out the first key enzyme, *Fld*, in the methanol dissimilation pathway of strain GS115. The resulting dissimilation pathway-blocking strain,  $\Delta$ FLD, exhibited pronounced growth defects in methanol-containing medium compared to the control strain GS115. Transcriptome analysis indicated that the blocked

dissimilation pathway led to the downregulation of the assimilation pathway.

In this study, we aimed to improve the utilization of methanol in strain  $\Delta$ FLD through metabolic pathway modification. Our investigation revealed that the growth defect in strain  $\Delta$ FLD was partially attributed to the excessive accumulation of formaldehyde and a decrease in the NAD<sup>+</sup>/NADH ratio in the presence of methanol. Consequently, we focused on reducing formaldehyde accumulation and increasing the NAD<sup>+</sup>/NADH ratio to improve methanol utilization in strain  $\Delta$ FLD (Fig. 1). To address the toxicity of formaldehyde, we implemented strategies such as limiting formaldehyde diffusion through the self-assembly of key enzymes *Aox1* and *Das1* involved in methanol metabolism. Additionally, we promoted formaldehyde assimilation by augmenting the amount of formaldehyde co-reactive substrate, Xu5P. In order to increase the NAD<sup>+</sup>/NADH ratio, NADH production was primarily increased by overexpression of the isocitrate dehydrogenase (*Idh*) in the TCA cycle. Simultaneously, we facilitated intracellular NADH translocation to mitochondria by increasing the amount of malate dehydrogenase (*Mdh*) in the malate-aspartate shuttle (also known as malate shuttle) system. Furthermore, the heterologous expression of methanol oxidase (*Mox*) from *Hansenula polymorpha* was introduced to improve the methanol utilization capacity and growth of the strain in 3% high concentration methanol. In this study, the efficient utilization strategy of methanol provided a valuable base for the application of *K. phaffii* in industrial biotechnology.

## Materials and methods

### Construction of plasmids and strains

The plasmids and strains constructed in this study are listed in Tables 1 and 2.

Strain construction was performed with plasmid-based expression, and plasmids were constructed using the Gibson Assembly Master Mix. All overexpressed genes were performed under the P<sub>AOX1</sub> using PPIC9K or PPICZA as vector backbone, purchased from Invitrogen (Carlsbad, CA, USA). Genes such as *AOX1*, *DAS1*, *FBA* (PAS\_chr1-1\_0319), *FBP* (PAS\_chr3\_0868), *TAL* (PAS\_chr2-2\_0338), *RPIA* (PAS\_chr4\_0212), *DAK* (PAS\_chr3\_0841), *MDH* (PAS\_chr4\_0815), *IDH* (PAS\_chr2-1\_0120) were amplified by PCR from the genome of *K. phaffii*.

The plasmids were introduced into *K. phaffii* cells by electroporation, using an Eppendorf Eporator (Eppendorf, Germany).

### Media and strain cultivation

*Escherichia coli* Top10 was used as the host strain for the amplification of plasmid. The strains were grown at 37 °C and 250 rpm in lysogeny broth (LB) medium (1%



**Table 1** Plasmids used in this study

Plasmids	Genotype	Source or reference
PPIC9K	Kan <sup>R</sup>	Invitrogen
PPICZA	Zeocin <sup>R</sup>	Invitrogen
PPICKSTD	Kan <sup>R</sup> , P <sub>AOX1</sub> -Spytag-Das1-T <sub>AOX1</sub>	This study
PPICZSCA	Zeocin <sup>R</sup> ; P <sub>AOX1</sub> -Cre-T <sub>AOX1</sub> ; P <sub>AOX1</sub> -Spycather-Aox1-T <sub>AOX1</sub>	This study
PHKAM	Kan <sup>R</sup> , P <sub>AOX1</sub> -MDH-T <sub>AOX1</sub>	This study
PHKAI	Kan <sup>R</sup> , P <sub>AOX1</sub> -IDH-T <sub>AOX1</sub>	This study
PHKAP	Kan <sup>R</sup> , P <sub>AOX1</sub> -FBP-T <sub>AOX1</sub>	This study
PHKAA	Kan <sup>R</sup> , P <sub>AOX1</sub> -FBA-T <sub>AOX1</sub>	This study
PHKAD	Kan <sup>R</sup> , P <sub>AOX1</sub> -DAK-T <sub>AOX1</sub>	This study
PHKAT	Kan <sup>R</sup> , P <sub>AOX1</sub> -TAL-T <sub>AOX1</sub>	This study
PHKAR	Kan <sup>R</sup> , P <sub>AOX1</sub> -RPIA-T <sub>AOX1</sub>	This study
PPICZAG	Zeocin <sup>R</sup> , P <sub>AOX1</sub> -based expression vector;	This study
PPICZAGMP	Zeocin <sup>R</sup> , P <sub>AOX1</sub> -MDH-T <sub>AOX1</sub> ; P <sub>AOX1</sub> -FBP-T <sub>AOX1</sub>	This study
PPICZAGIP	Zeocin <sup>R</sup> , P <sub>AOX1</sub> -IDH-T <sub>AOX1</sub> ; P <sub>AOX1</sub> -FBP-T <sub>AOX1</sub>	This study
PPICZAGMIP	Zeocin <sup>R</sup> , P <sub>AOX1</sub> -MDH-T <sub>AOX1</sub> ; P <sub>AOX1</sub> -IDH-T <sub>AOX1</sub> ; P <sub>AOX1</sub> -FBP-T <sub>AOX1</sub>	This study
PPICZAGIMOX	Zeocin <sup>R</sup> , P <sub>AOX1</sub> -IDH-T <sub>AOX1</sub> ; P <sub>AOX1</sub> -FBP-T <sub>AOX1</sub> ; P <sub>AOX1</sub> -MOX-T <sub>AOX1</sub>	This study

**Table 2** Strains used in this study

Strain	Genotype	Source or reference
<b><i>E. coli</i></b>		
TOP 10	Wild type	Invitrogen
<b><i>K. phaffii</i></b>		
GS115	<i>HIS4</i> <sup>-</sup>	Invitrogen
ΔFLD	GS115, ΔFLD	Lab conserved [15]
DF00	GS115, ΔFLD, <i>HIS4</i> <sup>+</sup>	This study
DF01	GS115, ΔFLD, <i>HIS4</i> <sup>+</sup> , <i>Spytag-DAS1</i>	This study
DF02	GS115, ΔFLD, <i>HIS4</i> <sup>+</sup> , <i>Spytag-DAS1</i> , <i>Spycather-AOX1</i>	This study
DF03	GS115, ΔFLD, <i>HIS4</i> <sup>+</sup> , <i>FBA</i>	This study
DF04	GS115, ΔFLD, <i>HIS4</i> <sup>+</sup> , <i>DAK</i>	This study
DF05	GS115, ΔFLD, <i>HIS4</i> <sup>+</sup> , <i>FBP</i>	This study
DF06	GS115, ΔFLD, <i>HIS4</i> <sup>+</sup> , <i>RPIA</i>	This study
DF07	GS115, ΔFLD, <i>HIS4</i> <sup>+</sup> , <i>TAL</i>	This study
DF08	GS115, ΔFLD, <i>HIS4</i> <sup>+</sup> , <i>IDH</i>	This study
DF09	GS115, ΔFLD, <i>HIS4</i> <sup>+</sup> , <i>MDH</i>	This study
DF10	GS115, ΔFLD, <i>HIS4</i> <sup>+</sup> , <i>MDH</i> , <i>IDH</i>	This study
DF02-1	DF02, <i>HIS4</i> <sup>+</sup> , <i>IDH</i> , <i>FBP</i>	This study
DF02-2	DF02, <i>HIS4</i> <sup>+</sup> , <i>MDH</i> , <i>FBP</i>	This study
DF02-3	DF02, <i>HIS4</i> <sup>+</sup> , <i>MDH</i> , <i>IDH</i> , <i>FBP</i>	This study
DF02-4	DF02, <i>HIS4</i> <sup>+</sup> , <i>IDH</i> , <i>FBP</i> , <i>MOX</i>	This study

### Methanol assay

Methanol concentration was determined by high performance liquid chromatography [16]. A 1 mL sample from the fermentation was centrifuged at 6000 rpm for 5 min and the supernatant was filtered through a 0.2 μm filter

using a syringe and analyzed on an LC-16 high performance liquid chromatograph (Shimadzu) equipped with a differential refractive index detector (RID-20 A) using a CarboMix H-NP10: 8% column (Sepax Technologies, Inc.). The samples were eluted with 2.5 mM H<sub>2</sub>SO<sub>4</sub> at a flow rate of 0.6 mL/min at 55 °C for 25 min.

### Formaldehyde assay

Formaldehyde was assayed during growth through the colorimetric Nash assay [17]. 1 mL of sample was centrifuged at 6000 rpm for 5 min. 100 μL of supernatant was pipetted into a 96-well plate (make three replicate wells for each sample), and then 100 μL of Nash reagent [10] (5 M ammonium acetate, 50 mM acetylacetone, and 135 mM acetic acid) was pipetted to mix. The mixture was incubated at 37 °C for 1 h. The absorbance was measured at 412 nm using a microtiter plate reader BioTek Synergy H1 (BioTek). The concentrations were calculated based on a standard curve, freshly prepared with the same batch of the test.

### ROS assay

The cellular ROS level was estimated by using the oxidant sensitive probe 2',7'-dichlorofluorescein diacetate (DCFH-DA) as described previously [18]. Samples were collected and washed twice with PBS (pH 7.4). The cells were then resuspended in 1 mL 10 mM PBS (pH 7.4) containing 10 μM DCFH-DA, and incubated at 37 °C for 1 h. Fluorescence was measured at λEX 485 nm and λEM 525 nm.

### Measurement of NAD<sup>+</sup>/NADH ratio

The NAD<sup>+</sup>/NADH ratio was assayed using the NAD<sup>+</sup>/NADH Assay Kit with WST-8 from Beyotime (Nantong, China). Following the removal of the medium by centrifugation, 1 mL of pre-cooled lysis buffer was added to the cells, and complete extraction was achieved by breaking the cells with glass beads. Subsequently, the mixtures were centrifuged at 4 °C for 10 min at 12,000 rpm. The supernatant samples were divided into two tubes of 100 μL each and used to measure NADH and total intracellular NAD. Finally, NAD<sup>+</sup>/NADH was measured and calculated according to the manufacturer's protocol [19]. The protein concentration was measured by the Bradford method [20]. All fluorescence intensity was normalized to the protein level of the supernatant.

### Measurement of propidium iodide (PI) staining

The method of PI staining refers to the previous studies in our laboratory [21]. The cells were collected at 6,000 rpm for 1 min, washed three times in 10 mM phosphate-buffered saline (PBS, pH 7.4). Then, a 10-μL aliquota of 5 mM propidium iodide (PI) was added to 200 μL cell suspension and incubated on a shaker for 30 min at 37 °C. The cells were washed three times and resuspended in 1.5 mL

PBS (pH 7.4). One hundred thousand cells per sample were counted and analyzed by flow cytometry (Beckman Coulter, Fullerton, CA, USA). The data was analyzed by software FlowJo v10.8.1.

### RNA isolation and RT-qPCR

The transcription levels of genes were analyzed by qRT-PCR. Total RNA was extracted from GS115 strains grown in BMMY for 24 h using the hot acid phenol method [22]. For the synthesis of cDNA, PrimeScript™ RT kit from Takara and gDNA Eraser (Perfect Real-time) were used according to the manufacturer's instructions, and 1 µg of total RNA was used as the template [18]. The mRNA was quantified by qRT-PCR using TB Green® Premix Ex Taq™ (Takara, Japan) [23]. Glyceraldehyde-3-phosphate dehydrogenase gene GAPDH was selected as the house-keeping gene. The primers of RT-qPCR used in this study are listed in Table 2. All experiments were carried out independently in triplicate. The expression ratio of a gene was analyzed by  $2^{-\Delta\Delta C_t}$  method [24].

## Results and discussion

### Weak growth of $\Delta$ FLD in methanol

In the dissimilation pathway of methanol metabolism in *K. phaffii*, formaldehyde undergoes initial oxidized by Fld and Fgh to formic acid, subsequently further oxidized to CO<sub>2</sub> [25]. During the dissimilation of formaldehyde,

the conversion of 1 molecule of formaldehyde is coupled with the transformation of 2 molecules of NAD<sup>+</sup> to NADH. However, excessive dissimilation of methanol leads to a significant loss of C1 substrate in the form of CO<sub>2</sub>, thereby endangering the yield of biomass and target chemicals and reducing the economics of the methanol carbon atom [26]. In the previous research, a strain  $\Delta$ FLD with a blocked dissimilation pathway was generated [15]. The  $\Delta$ FLD strain exhibited severe growth defects in medium containing 1% methanol and demonstrated limited methanol utilization (Fig. 2A and C).

Through the experiment, we found that there was a large amount of formaldehyde accumulated in the supernatant of the fermentation broth of the  $\Delta$ FLD strain, with the accumulated formaldehyde levels being 2~3 times higher than those in the control strain GS115 (Fig. 2B). Formaldehyde is known to be non-specifically toxic to intracellular DNA and proteins [27]. Strains of *K. phaffii* with compromised integrity face challenges in normal growth in medium where methanol serves as the carbon source, similar to the trend of inhibition of the assimilation pathway due to knockdown of the dissimilation pathway found in previous studies [15]. Measurement of intracellular NAD<sup>+</sup>/NADH, it was found that the intracellular NAD<sup>+</sup>/NADH revealed a lower ratio in the  $\Delta$ FLD strain compared to GS115 (Fig. 2D). As a cofactor, NAD (NAD<sup>+</sup> and NADH) participates in over 300 intracellular

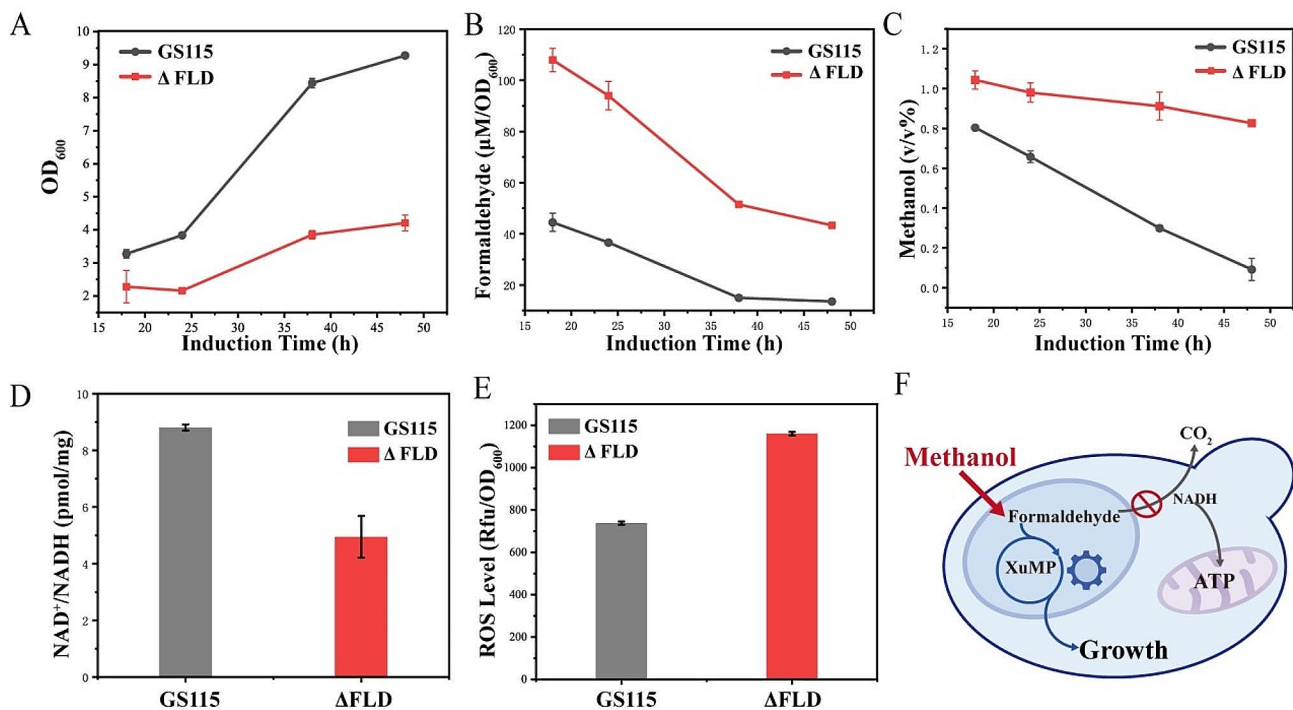


**Fig. 2** A comparison between strains  $\Delta$ FLD and GS115 in 25 mL of BMMY medium with 1% methanol. **A** Measurement of growth curve; The x-axes of the culture plots start at 18 h. **B** Measurement of fermentation supernatant formaldehyde; **C** Measurement of fermentation supernatant methanol; **D** Measurement of intracellular NAD<sup>+</sup>/NADH; **E** Measurement of intracellular ROS; **F** Schematic diagram of strain  $\Delta$ FLD. Error bars represent the standard deviation of 2 or 3 biological replicates

redox reactions, playing an important role in cellular metabolism [28]. The imbalance in the supply of  $\text{NAD}^+$ / $\text{NADH}$  caused disrupted intracellular metabolism, affecting the growth of the *K. phaffii* strain in methanol. The methanol dissimilation pathway is a rapid metabolic pathway for the toxic substance formaldehyde and a source of  $\text{NADH}$  and  $\text{ATP}$  [29, 30]. Impairment of the dissimilation pathway led to formaldehyde accumulation and intracellular  $\text{NAD}$  disruption, causing increased intracellular ROS levels (Fig. 2E), which affected methanol metabolism in microbial cell factories. Hence, our studies focused on improving the utilization of methanol by the  $\Delta\text{FLD}$  strain by reducing formaldehyde accumulation and increasing  $\text{NAD}$  balance.

### Reduction of formaldehyde diffusion by self-assembly of Aox1 and Das1

The excessive accumulation of formaldehyde exerts a toxic effect on proteins and nucleic acids, impeding the efficient utilization of methanol by strains. Therefore, the swift metabolism of formaldehyde is crucial to enhance methanol utilization in strains. Fan [31] et al. fused and expressed Mdh, Hps and Phi in Synthetic methanotropic *E. coli* by flexible linker  $(\text{GGGGS})_n$ , resulting in improved methanol biotransformation. Thus, preventing

the diffusion of toxic intermediates into other intracellular pathways by improving the spatial proximity of enzymes in cascade reactions and the construction of substrate channels through enzyme complexes [32], offering be a promising strategy for enhancing methanol biotransformation [3].

Methanol is oxidized to formaldehyde by Aox in *K. phaffii*, and formaldehyde is further catalyzed by Das in the carbon metabolism assimilation pathway. Aox and Das are two key enzymes for methanol assimilation. Intracellular assembly of Aox1 and Das1 was performed using the protein scaffold Spycather/Spycather in the strain  $\Delta\text{FLD}$ , with Spycather attached to the C-terminus of Aox1 and Spycather attached to the C-terminus of Das1. Experimental results revealed that, in 1% methanol, the  $\text{OD}_{600}$  of the recombinant strain DF02 at 48 h was 2.15 times higher than that of DF00 ( $\Delta\text{FLD}$  back-complemented  $\text{HIS4}^+$ ) (Fig. 3A). Notably, assembled strain DF02 exhibited a similar methanol utilization capacity compared to unassembled strains DF00 and DF01 (Fig. 3B). However, DF02 demonstrated superior growth and lower formaldehyde accumulation, with a nearly 52.6% decrease in formaldehyde accumulation in the fermentation supernatant compared to DF00 (Fig. 3C). These results showed that the supramolecular enzyme complex

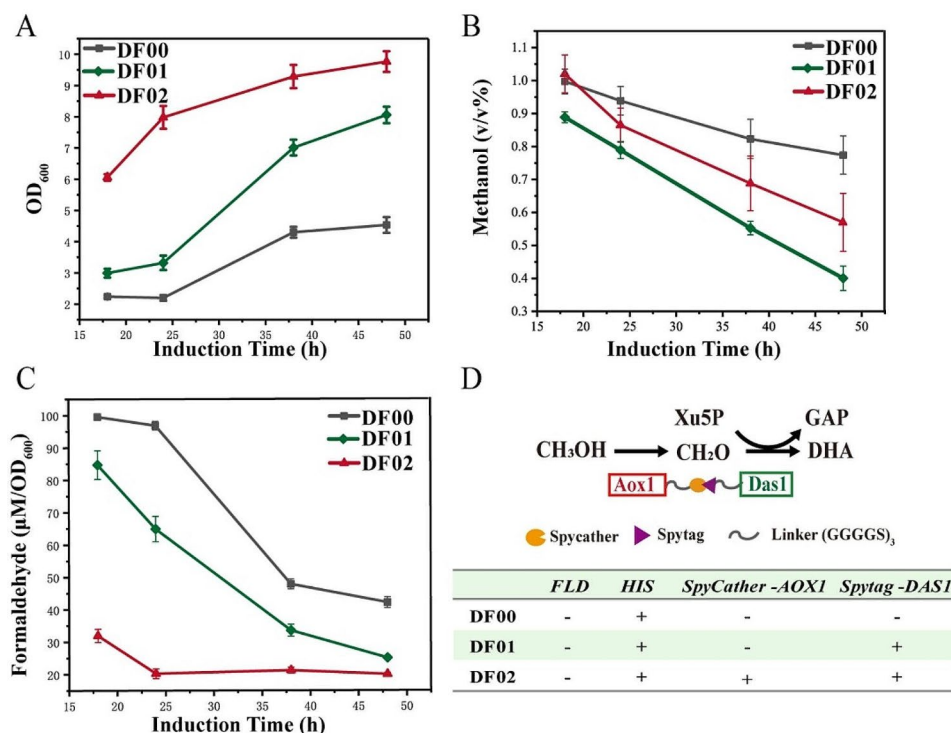


**Fig. 3** Analysis of strains with the Aox1/Das1 dual enzyme assembly strategy was incubated in 25 mL of BMMY medium containing 1% methanol. **A** Measurement of growth curve; The x-axes of the culture plots start at 18 h. **B** Measurement of fermentation supernatant formaldehyde; **C** Measurement of fermentation supernatant methanol; **D** Schematic diagram of double enzyme assembly. Aox, alcohol oxidase; Das, dihydroxyacetone synthase; Dak, dihydroxyacetone kinase; GAP, glyceraldehyde 3-phosphate; DHA, dihydroxyacetone; Xu5P, xylulose 5-phosphate. Error bars represent the standard deviation of 2 or 3 biological replicates

formed by the self-assembly of Aox1 and Das1 helped reducing the diffusion and accumulation of formaldehyde in cells, thereby promoting the growth of the strain in methanol. Moreover, it also indicates that formaldehyde is more toxic than methanol and has a great inhibitory effect on cell growth.

#### Promoted formaldehyde assimilation by increased formaldehyde receptor Xu5P

In the process of methanol metabolism, the generated formaldehyde necessitates further metabolized with a co-reaction substrate. The metabolism of formaldehyde is constrained by the availability of the co-reaction substrate, making it imperative to enhance the regeneration of the formaldehyde receptor for efficient methanol assimilation. However, the regeneration of the formaldehyde receptor poses a significant barrier to formaldehyde assimilation. Woolston et al [13] found that activation of the SBPase pathway and reduction of GAPDH in the RuMP cycle significantly enhanced the regeneration of Ru5P.

In the methanol assimilation metabolic pathway of *K. phaffii*, it is necessary for formaldehyde to produce GAP and DHA of Xu5P catalyzed by Das. Consequently,

the metabolism of formaldehyde is also limited by the amount of receptor Xu5P. Comparative analysis of transcriptomic data (Table S1) based on  $\Delta$ FLD strains in glucose or methanol media showed a significant increase in transcript levels of *DAK*, *FBA2*, *FBP1*, *RPIA*, and *TAL2*, key enzymes of the Xu5P regeneration cycle pathway under methanol culture conditions. The intracellular distribution of these enzymes has been analyzed using online protein localization simulations [33], and most of these enzymes are located in peroxisomes (Table S2). This was in contrast to the previously reported notion of an independent set of non-oxidative phosphorylation pathways in peroxisomes to regenerate Xu5P [34].

Genes for these enzymes were amplified from the *K. phaffii* GS115 genome using PCR technology and overexpressed under the Aox1 methanol-induced promoter in the  $\Delta$ FLD strain (Fig. 4B). The engineered strains exhibited approximately 30% higher growth compared to the control strain DF00 (Fig. 4C), an increased methanol utilization rate (Fig. 4D), and reduced formaldehyde accumulation in methanol (Fig. 4E). Notably, strain DF05, overexpressing Fbp1, demonstrated a 32% increase in growth at 48 h and a 21.9% reduction in the accumulation of formaldehyde in the supernatant compared to the

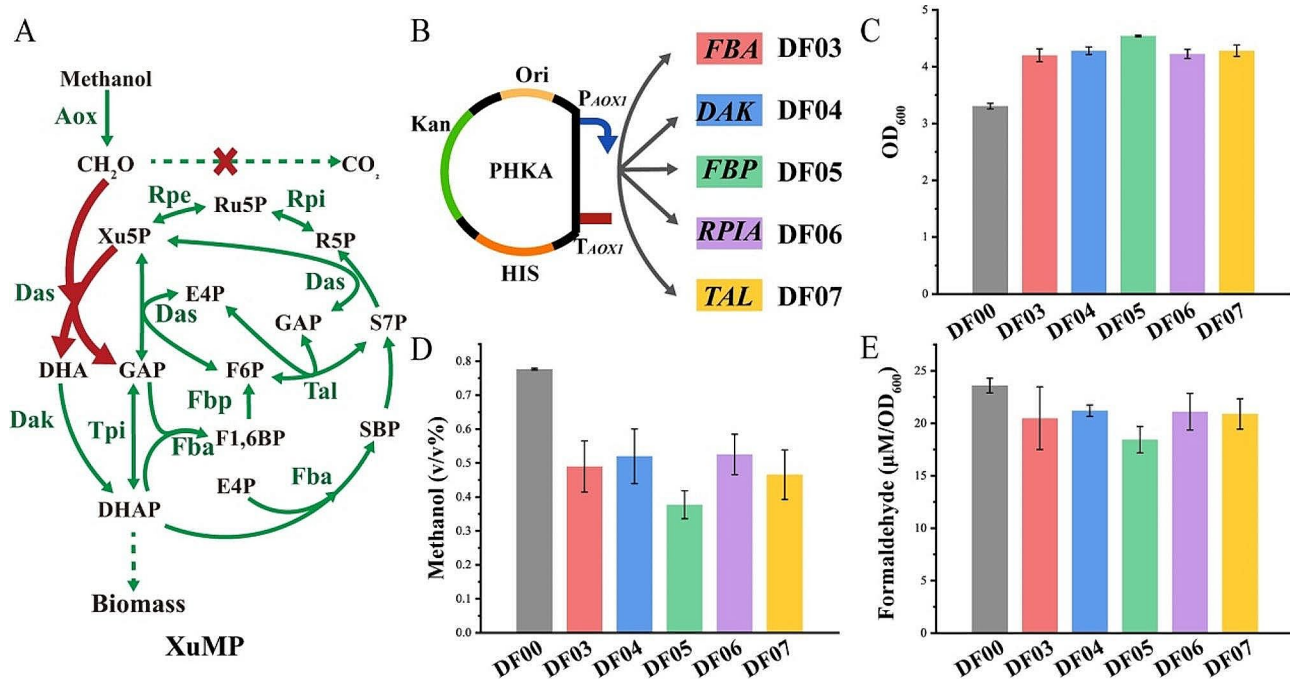


**Fig. 4** Analysis of strains with overexpression of key enzymes of the XuMP pathway were incubated in 25 mL of BMMY medium containing 1% methanol. **A** Schematic diagram of the methanol assimilation metabolic pathway, Aox, alcohol oxidase; Das, dihydroxyacetone synthase; Dak, dihydroxyacetone kinase; Fba fructose-bisphosphate aldolase; Fbp, fructose bisphosphatase; Tpi, triosephosphate isomerase; Tal, transaldolase; Rpi, ribose-5-phosphate isomerase; Rpe ribulose phosphate 3-epimerase; GAP, glyceraldehyde 3-phosphate; DHA, dihydroxyacetone; DHAP, dihydroxyacetone phosphate; F1,6BP, fructose-1,6-bisphosphate; F6P, fructose 6 phosphate; E4P, erythrose-4-phosphate; SBP, sedoheptulose 1,7-bisphosphate; S7P, sedoheptulose 7-phosphate; Xu5P, xylulose 5-phosphate; R5P, ribose 5-phosphate; Ru5P, ribulose 5-phosphate; **B** Schematic diagram of the overexpression plasmid; **C** Measurement of 48 h growth OD<sub>600</sub>; **D** Measurement of 48 h fermentation supernatant methanol; **E** Measurement of fermentation supernatant formaldehyde. Error bars represent the standard deviation of 2 or 3 biological replicates

control strain DF00, showcasing maximal enhancement in formaldehyde receptor regeneration.

### Optimization of intracellular $\text{NAD}^+/\text{NADH}$ balance promote strain growth

In methanol-grown methylotrophic yeast, cellular energy is primarily derived through two main pathways: the TCA cycle reaction via the respiratory chain and the methanol dissimilation pathway [35]. Within the dissimilation pathway, each molecule of formaldehyde is accompanied by 2 molecules of NADH production, which then passes  $\text{H}^+$  through the NADH shuttle system to the respiratory chain inside the mitochondria to produce ATP for cell growth [26, 36]. *FLD* knockdown resulted in a reduction in the intracellular  $\text{NAD}^+/\text{NADH}$  ratio. The  $\text{NAD}^+/\text{NADH}$  ratio in cells represents the redox state, which is influenced by and in turn regulates metabolic activity, and redox homeostasis is necessary for optimal cellular health throughout the life cycle [37, 38].

Overexpression of *Idh* in the TCA cycle and *Mdh* in the NADH malate transport shuttle system was performed individually and in combination in the  $\Delta\text{FLD}$  strain. Experimental results demonstrated improved intracellular  $\text{NAD}^+/\text{NADH}$  ratio and methanol utilization rates in 1% methanol, leading to a 30% increase in  $\text{OD}_{600}$  growth. The DF10 strain, expressing *Idh* and *Mdh*

in combination, exhibited the most substantial increase in  $\text{NAD}^+/\text{NADH}$  ratio, reaching approximately 10, followed by the DF08 strain expressing *Idh* (Fig. 5D). However, the growth and methanol utilization capabilities of DF10 strains were not as strong as DF08 strains (Fig. 5C and E), potentially linked to the metabolic stress tendency associated with strains expressing multiple proteins. After 48 h of incubation in 1% methanol, the strain DF08 increased the growth  $\text{OD}_{600}$  by 34.9% compared with the strain DF00 (Fig. 5C), and methanol residue in the fermentation supernatant decreased by nearly 33.9% ((Fig. 5E). Some studies have observed a decrease in the  $\text{NAD}^+/\text{NADH}$  ratio during cellular senescence [39, 40]. By enhancing the TCA cycle and NADH shuttle system, the intracellular  $\text{NAD}^+/\text{NADH}$  ratio can be optimized, improving the intracellular redox state, and promoting methanol utilization in  $\Delta\text{FLD}$  strains.

### Systematic metabolic modification portfolio to improve methanol utilization

According to the analysis of the results of the multi-strategy described above, the *Aox1/Das1* dual enzyme assembly strain DF02 underwent individual and combined overexpression of *FBP* (XuMP pathway), *IDH* (TCA cycle) and *MDH*. The results, shown in Fig. 6A, revealed that strain DF02-1 exhibited optimal growth

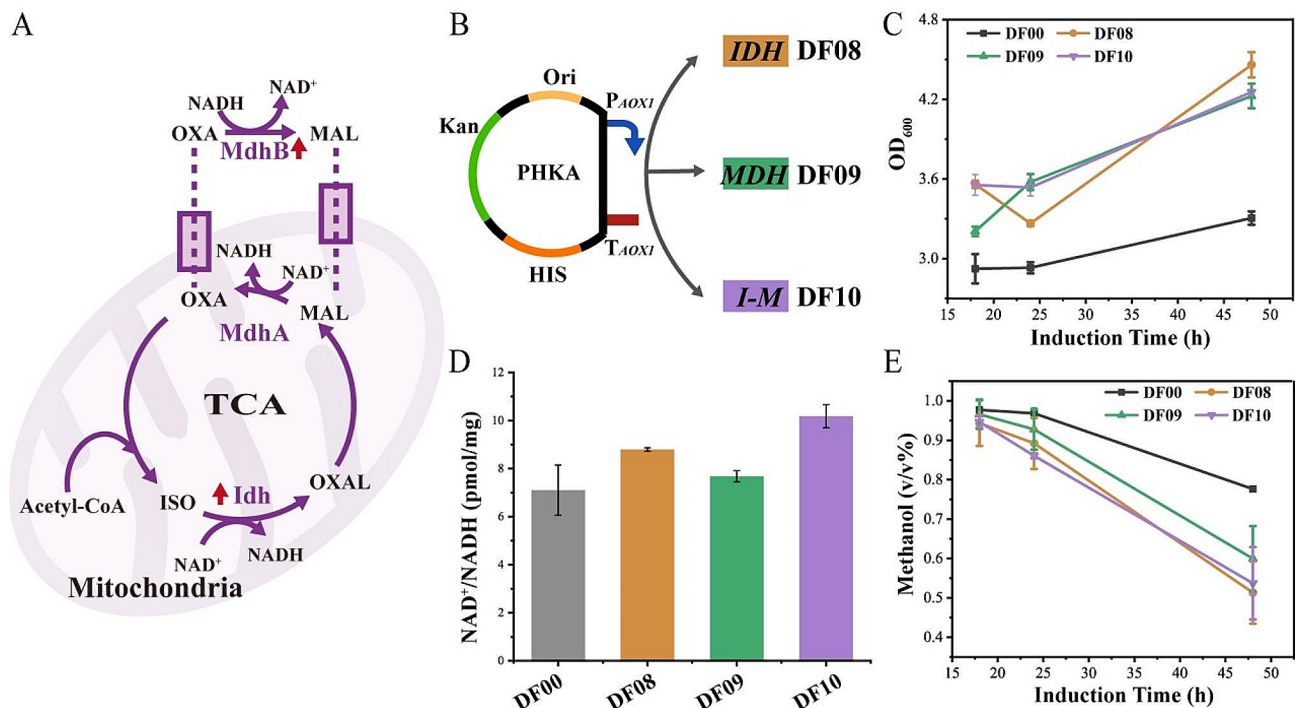


**Fig. 5** Analysis of strains with enzyme overexpression with  $\text{NAD}^+$  as cofactor was incubated in 25 mL of BMMY medium containing 1% methanol. **A** Schematic diagram of TCA cycle and malate shuttle system, Mdh, malate dehydrogenase; Idh, isocitrate dehydrogenase; MAL, malate; OXA, oxaloacetate; ISO, isocitrate; OXAL, oxalosuccinate; **B** Schematic diagram of expression plasmid; **C** Measurement of growth curve; The x-axes of the culture plots start at 18 h. **D** Measurement of intracellular  $\text{NAD}^+/\text{NADH}$ ; **E** Measurement of methanol in fermentation supernatant. Error bars represent the standard deviation of 2 or 3 biological replicates

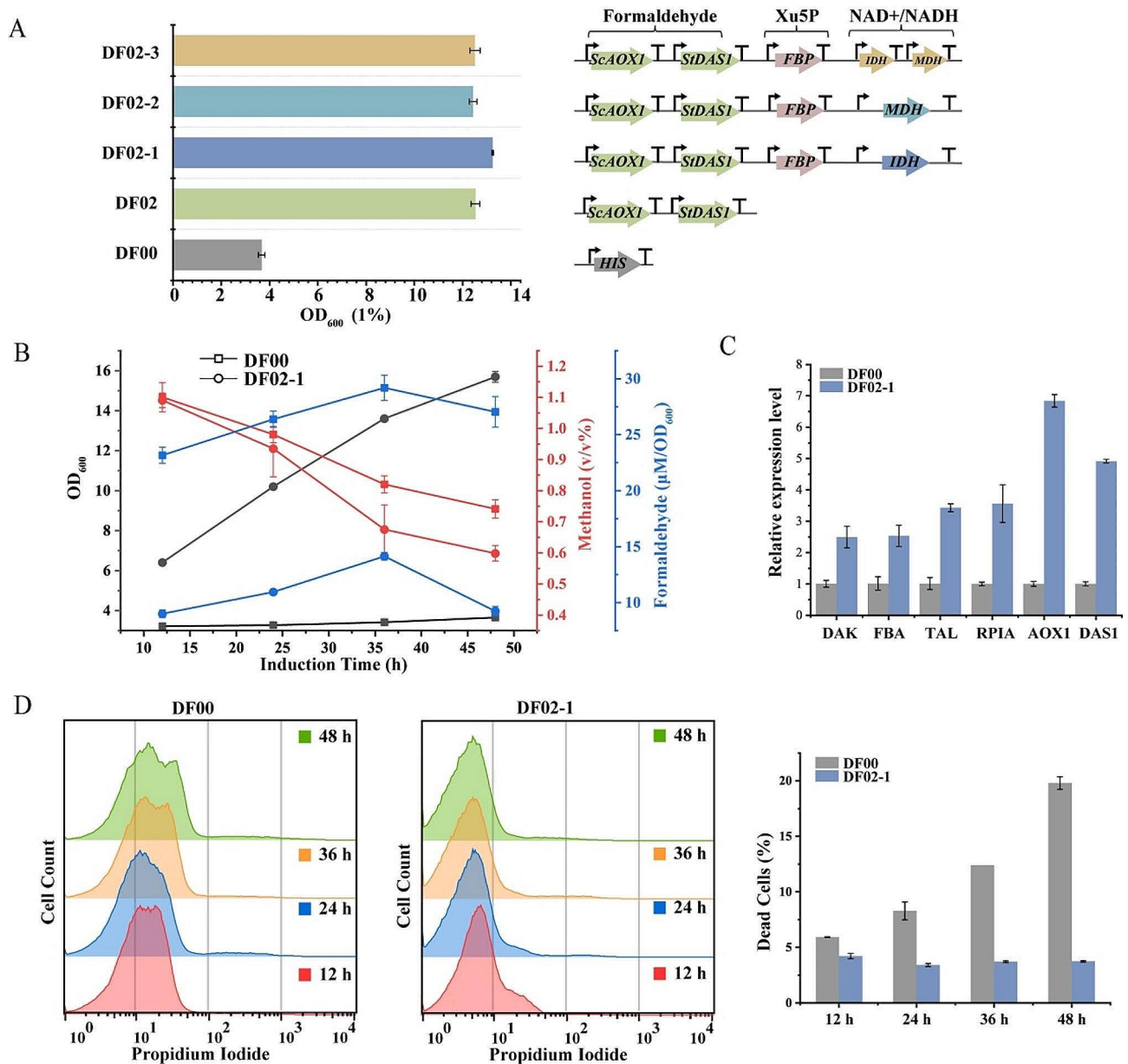


**Fig. 6** The analysis of strains with an integrated strategy was incubated in 25 mL of BMMY medium containing 1% methanol. **A** Growth  $OD_{600}$  of recombinant strains at 48 h; **B** Measurement of  $OD_{600}$ , methanol content and formaldehyde content of recombinant strains DF02-1 and DF00 grown in 1% methanol; The x-axes of the culture plots start at 12 h. **C** Transcript levels of key enzymes of methanol metabolism; **D** Mortality of recombinant strains in 1% methanol by flow cytometry. Error bars represent the standard deviation of 2 or 3 biological replicates

performance, with a 4.28-fold increase in  $OD_{600}$  over the DF00 control strain after 48 h in 1% methanol. In contrast, strains DF02-2 and DF02-3 displayed lower growth rates compared to DF02. Subsequent comparisons between the final strain DF02-1 and strain DF00 in 1% methanol (Fig. 6B) demonstrated a 20% reduction in methanol residue and a 65.7% decrease in formaldehyde accumulation in DF02-1, accompanied by a 81.1% reduction in cell death compared to DF00 at 48 h (Fig. 6D).

The observed excessive formaldehyde accumulation in the DF00 strain over time, attributed to the *FLD*

deletion, led to increased toxicity to cells. This, coupled with a decreased methanol utilization capacity, resulted in elevated methanol levels in the fermentation supernatant, contributing to the dual toxicity of methanol and formaldehyde and an escalating number of dead cells. Transcript levels analysis of key methanol metabolizing enzymes in strains DF00 and DF02-1 in 1% methanol (Fig. 6C) showed that the recombinant strain DF02-1 exhibited 2.5-7 times higher overall transcript levels of methanol metabolizing pathway genes compared to DF00. Notably, the overexpressed *FBP* and *IDH* genes in

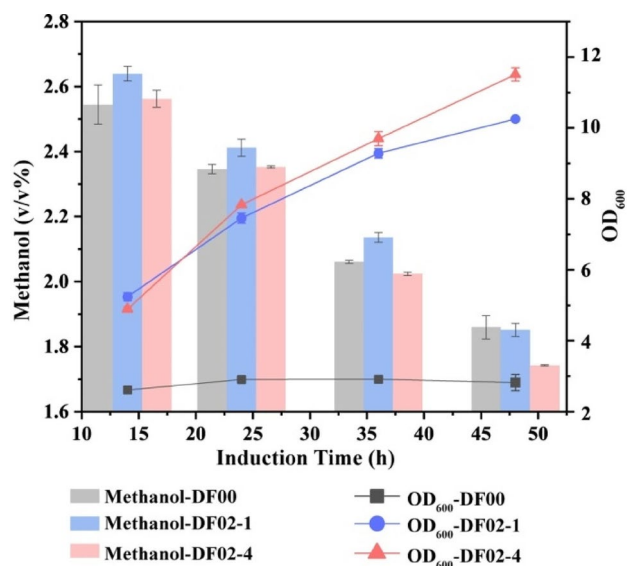


**Fig. 7** Analysis of recombinant strain DF02-4 in 3% methanol. Error bars represent the standard deviation of 2 or 3 biological replicates. The x-axes of the culture plots start at 14 h

DF02-1 showed 41.9 and 203.6 times higher transcript levels, respectively (Fig. S3).

In conclusion, the construction of the Aox1/Das1 dual enzyme assembly, along with enhanced Xu5P regeneration and increased intracellular  $NAD^+/NADH$ , successfully promoted methanol assimilation, leading to improved strain growth in methanol.

#### Improved utilization of high methanol concentrations in recombinant strain DF02-1

In order to determine the methanol utilization ability of recombinant strain DF02-1 in high concentrations of methanol, we found that the residual amount of methanol in the fermentation supernatant of strain DF02-1 and DF00 were similar in the medium containing 3% methanol, and the methanol utilization ability of the strain was impaired by high concentrations of methanol [35]. In previous studies [41], heterologous expression of *MOX* derived from *Hansenula polymorpha* in *K. phaffii* promoted the methanol utilization in high concentration methanol by recombinant strains. Here we heterologously expressed the enzyme Mox on the basis of the DF02-1 strain, and the designated recombinant strain DF02-4 further improved the utilization of methanol. In BMMY medium containing 3% methanol, the growth  $OD_{600}$  of DF02-4 incubated for 48 h was 1.12 times higher than that of DF02-1. At 48 h, the growth  $OD_{600}$  of DF02-4 was 4.08 times higher than that of the initial strain DF00, and methanol utilization increased by 10.26%. (Fig. 7). This result indicated that the heterologous expression of *MOX* could effectively improve the growth of the strain in 3% methanol and utilization of methanol.

## Conclusions

In a previous investigation [15], we knocked out the first important enzyme Fld in the dissimilation pathway to reduce the loss of methanol in the form of  $CO_2$  through the dissimilation pathway of *K. phaffii*. Transcriptomic and metabolomic analyses of the resulting strain  $\Delta FLD$  revealed a down-regulation in the assimilation pathway, elucidating the growth impairment observed in  $\Delta FLD$  when cultivated in methanol.

In this study, we analyzed the strain  $\Delta FLD$  in 1% methanol, revealing subpar methanol utilization, substantial formaldehyde accumulation, and a diminished intracellular  $NAD^+/NADH$  ratio. To address these issues, we employed a multifaceted approach. We assembled Aox1 and Das1 into multifunctional enzyme complexes using the Spytag/Spycather protein scaffold, creating substrate channels to reduce formaldehyde diffusion within the cell. Simultaneously, we augmented the catalytic rate of formaldehyde and enhanced Xu5P regeneration by overexpressing key enzymes in the XuMP pathway, thereby fostering strain growth in methanol and mitigating formaldehyde accumulation. Notably, the  $NAD^+/NADH$  ratio determines the metabolic fluxes of many intracellular pathways and the transcription levels of many genes [28]. As expected, the strategy of overexpressing *IDH* of the TCA cycle and *MDH* of the malate transport shuttle system improved the growth of the strain in methanol and the  $NAD^+/NADH$  ratio. The high concentration methanol weakened the methanol utilization capacity of the strain, nevertheless, the heterologous expression of *MOX* could improve the transformation of methanol by the strain.

Ultimately, by combining multiple strategies—Aox1/Das1 double enzyme assembly, overexpression of Fbp in the XuMP pathway, Idh in the TCA cycle, and heterologous expression of *MOX*—the resulting recombinant strain DF02-4 exhibited a remarkable  $OD_{600}$ , 4.08 times higher than that of the  $\Delta FLD$  strain in a medium with 3% methanol. These findings establish a solid research foundation for achieving the economic and efficient utilization of methanol in *K. phaffii*.

## Supplementary Information

The online version contains supplementary material available at <https://doi.org/10.1186/s12934-024-02475-1>.

Supplementary Material 1

## Acknowledgements

Not applicable.

## Author contributions

YY.W: Conceptualization, Methodology, Investigation, Writing, Visualization. RS.L: Investigation, Writing, Visualization. FG.Z: Methodology, Investigation. S.W: Methodology. YP.Z: Methodology. DX. F: Writing. SY.H: Conceptualization, Supervision, Review and Editing, Funding acquisition.

### Funding

This work was supported by the National Key R&D Program of China (2022YFC2105501).

### Data availability

No datasets were generated or analysed during the current study.

### Declarations

#### Ethics approval and consent to participate

Not applicable.

#### Consent for publication

Not applicable.

#### Competing interests

The authors declare no competing interests.

Received: 25 April 2024 / Accepted: 8 July 2024

Published online: 17 July 2024

### References

- Bertau M, Offermanns H, Plass L, Schmidt F, Wernicke HJ. *Methanol: The Basic Chemical and Energy Feedstock of the Future* 2014.
- Du XL, Jiang Z, Su DS, Wang JQ. Research Progress on the Indirect Hydrogenation of Carbon Dioxide to methanol. *Chemsuschem*. 2016;9:322–32.
- Wang Y, Fan L, Tuyishime P, Zheng P, Sun J. Synthetic methylotrophy: a practical solution for methanol-based Biomanufacturing. *Trends Biotechnol*. 2020;38:650–66.
- Bennett RK, Gonzalez JE, Whitaker WB, Antoniewicz MR, Papoutsakis ET. Expression of heterologous non-oxidative pentose phosphate pathway from *Bacillus methanolicus* and phosphoglucose isomerase deletion improves methanol assimilation and metabolite production by a synthetic *Escherichia coli* methylotroph. *Metab Eng*. 2018;45:75–85.
- Whitaker WB, Sandoval NR, Bennett RK, Fast AG, Papoutsakis ET. Synthetic methylotrophy: engineering the production of biofuels and chemicals based on the biology of aerobic methanol utilization. *Curr Opin Biotechnol*. 2015;33:165–75.
- Antoniewicz MR. Synthetic methylotrophy: strategies to assimilate methanol for growth and chemicals production. *Curr Opin Biotechnol*. 2019;59:165–74.
- Gonzalez JE, Bennett RK, Papoutsakis ET, Antoniewicz MR. Methanol assimilation in *Escherichia coli* is improved by co-utilization of threonine and deletion of leucine-responsive regulatory protein. *Metab Eng*. 2018;45:67–74.
- Tuyishime P, Wang Y, Fan LW, Zhang QQ, Li QG, Zheng P, Sun JB, Ma YH. Engineering *Corynebacterium glutamicum* for methanol-dependent growth and glutamate production. *Metab Eng*. 2018;49:220–31.
- Dai ZX, Gu HL, Zhang SJ, Xin FX, Zhang WM, Dong WL, Ma JF, Jia HH, Jiang M. Metabolic construction strategies for direct methanol utilization in *Saccharomyces cerevisiae*. *Bioresour Technol*. 2017;245:1407–12.
- Wang GK, Olofsson-Dolk M, Hansson FG, Donati S, Li XL, Chang H, Cheng J, Dahlin J, Borodina I. Engineering yeast *Yarrowia lipolytica* for methanol assimilation. *ACS Synth Biol*. 2021;10:3537–50.
- Kurtzman CP. Biotechnological strains of *Komagataella (Pichia) pastoris* are *Komagataella Phaffii* as determined from multigene sequence analysis. *J Ind Microbiol Biotechnol*. 2009;36:1435–8.
- Vanz AL, Lunsdorf H, Adnan A, Nimtz M, Gurramkonda C, Khanna N, Rinas U. Physiological response of *Pichia pastoris* GS115 to methanol-induced high level production of the Hepatitis B surface antigen: catabolic adaptation, stress responses, and autophagic processes. *Microb Cell Fact* 2012, 11.
- Woolston BM, King JR, Reiter M, Van Hove B, Stephanopoulos G. Improving formaldehyde consumption drives methanol assimilation in engineered *E. Coli*. *Nat Commun* 2018, 9.
- Cai P, Wu X, Deng J, Gao L, Shen Y, Yao L, Zhou YJ. Methanol biotransformation toward high-level production of fatty acid derivatives by engineering the industrial yeast *Pichia pastoris*. *Proc Natl Acad Sci U S A*. 2022;119:e2201711119.
- Yu YF, Yang J, Zhao F, Lin Y, Han S. Comparative transcriptome and metabolome analyses reveal the methanol dissimilation pathway of *Pichia pastoris*. *BMC Genomics*. 2022;23:366.
- Wang D, Chen M, Zeng X, Li W, Liang S, Lin Y. Improving the catalytic performance of *Pichia pastoris* whole-cell biocatalysts by fermentation process. *RSC Adv*. 2021;11:36329–39.
- Rohlhill J, Gerald Har JR, Antoniewicz MR, Papoutsakis ET. Improving synthetic methylotrophy via dynamic formaldehyde regulation of pentose phosphate pathway genes and redox perturbation. *Metab Eng*. 2020;57:247–55.
- Lin NX, He RZ, Xu Y, Yu XW. Oxidative stress tolerance contributes to heterologous protein production in *Pichia pastoris*. *Biotechnol Biofuels*. 2021;14:160.
- Li CG, Zeng QZ, Chen MY, Xu LH, Zhang CC, Mai FY, Zeng CY, He XH, Ouyang DY. Evodiamine augments NLRP3 inflammasome activation and anti-bacterial responses through inducing alpha-tubulin acetylation. *Front Pharmacol*. 2019;10:290.
- Bradford MM. A rapid and sensitive method for the quantitation of microgram quantities of protein utilizing the principle of protein-dye binding. *Anal Biochem*. 1976;72:248–54.
- Wang D, Li W, Zhang X, Liang S, Lin Y. Green process: improved semi-continuous fermentation of *Pichia pastoris* based on the Principle of Vitality Cell separation. *Front Bioeng Biotechnol*. 2021;9:777774.
- Collart MA, Oliviero S. Preparation of yeast RNA. *Curr Protoc Mol Biol* 1993, 23:13.12.11–13.12.15.
- Zou C, Wang P, Liang S, Lin Y. Deletion of Gcw13 represses autophagy in *Pichia pastoris* cells grown in methanol medium with sufficient amino acids. *Biotechnol Lett*. 2019;41:1423–31.
- Jie H, Qi F, Liu H, Zou H, Ahmed MS, Li C. Novel helper factors influencing recombinant protein production in *Pichia pastoris* based on proteomic analysis under simulated microgravity. *Appl Microbiol Biotechnol*. 2015;99:653–65.
- Berrios J, Theron CW, Steels S, Ponce B, Velastegui E, Bustos C, Altamirano C, Fickers P. Role of Dissimilative Pathway of *Komagataella phaffii (Pichia pastoris)*: Formaldehyde Toxicity and Energy Metabolism. *Microorganisms* 2022, 10.
- Guo F, Qiao Y, Xin F, Zhang W, Jiang M. Bioconversion of C1 feedstocks for chemical production using *Pichia pastoris*. *Trends Biotechnol* 2023.
- Patterson JA, He H, Folz JS, Li Q, Wilson MA, Fiehn O, Bruner SD, Bar-Even A, Hanson AD. Thioproline formation as a driver of formaldehyde toxicity in *Escherichia coli*. *Biochem J*. 2020;477:1745–57.
- Zhou Y, Wang L, Yang F, Lin X, Zhang S, Zhao ZK. Determining the extremes of the cellular NAD(H) level by using an *Escherichia coli* NAD(+)-auxotrophic mutant. *Appl Environ Microbiol*. 2011;77:6133–40.
- Zhu T, Zhao T, Bankefa OE, Li Y. Engineering unnatural methylotrophic cell factories for methanol-based biomanufacturing: challenges and opportunities. *Biotechnol Adv*. 2020;39:107467.
- Zhan C, Li X, Yang Y, Nielsen J, Bai Z, Chen Y. Strategies and challenges with the microbial conversion of methanol to high-value chemicals. *Biotechnol Bioeng*. 2021;118:3655–68.
- Fan LW, Wang Y, Tuyishime P, Gao N, Li QG, Zheng P, Sun JB, Ma YH. Engineering Artificial Fusion proteins for enhanced methanol Bioconversion. *ChemBioChem*. 2018;19:2465–71.
- Dueber JE, Wu GC, Malmirchegini GR, Moon TS, Petzold CJ, Lullal AV, Prather KL, Keasling JD. Synthetic protein scaffolds provide modular control over metabolic flux. *Nat Biotechnol*. 2009;27:753–9.
- Farré JC, Li P, Subramani S. BiFC Method based on Intraorganellar Protein Crowding detects oleate-dependent Peroxisomal targeting of *Pichia pastoris* Malate Dehydrogenase. *Int J Mol Sci* 2021, 22.
- Rußmayer H, Buchetics M, Gruber C, Valli M, Grillitsch K, Modarres G, Guerraio R, Klavins K, Neubauer S, Drexler H, et al. Systems-level organization of yeast methylotrophic lifestyle. *BMC Biol*. 2015;13:80.
- Cai HL, Doi R, Shimada M, Hayakawa T, Nakagawa T. Metabolic regulation adapting to high methanol environment in the methylotrophic yeast *Ogataea methanolica*. *Microb Biotechnol*. 2021;14:1512–24.
- Eto K, Suga S, Wakui M, Tsubamoto Y, Terauchi Y, Taka J, Aizawa S, Noda M, Kimura S, Kasai H, Kadowaki T. NADH Shuttle System regulates KATPChannel-dependent pathway and steps distal to cytosolic Ca<sup>2+</sup> + concentration elevation in glucose-induced insulin Secretion\*. *J Biol Chem*. 1999;274:25386–92.
- Fahy GM, Brooke RT, Watson JP, Good Z, Vasanawala SS, Maecker H, Leipold MD, Li DTS, Kobor MS, Horvath S. Reversal of epigenetic aging and immunosenescence trends in humans. *Aging Cell* 2019, 18.
- Zhang ZG, Xu HN, Li SY, Davila A, Chellappa K, Davis JG, Guan YX, Frederick DW, Chu WQ, Zhao HQ, et al. Rapamycin maintains NAD(+)/NADH redox homeostasis in muscle cells. *Aging-Us*. 2020;12:17786–99.
- Zhu XH, Lu M, Lee BY, Ugurbil K, Chen W. In vivo NAD assay reveals the intracellular NAD contents and redox state in healthy human brain and their age dependences. *Proc Natl Acad Sci U S A*. 2015;112:2876–81.

40. Zhang Z, Xu HN, Li S Jr, Chellappa AD, Davis K, Guan JG, Frederick Y, Chu DW, Zhao W. Rapamycin maintains NAD(+)/NADH redox homeostasis in muscle cells. *Aging*. 2020;12:17786–99.
41. Wang YY, Li JW, Zhao FG, Zhang YP, Yang XR, Lin Y, Han SY. Methanol oxidase from *Hansenula polymorpha* shows activity in peroxisome-deficient *Pichia pastoris*. *Biochem Eng J* 2022, 180.

### **Publisher's Note**

Springer Nature remains neutral with regard to jurisdictional claims in published maps and institutional affiliations.